Plasmonics (2014) 9:537–544
DOI 10.1007/s11468-013-9656-1

Numerical Study of Optical Behavior of Nano-Hole Array with Non-Vertical Sidewall Profile

Mehrdad Irannejad · Jian Zhang · Mustafa Yavuz · Bo Cui

Received: 26 September 2013 / Accepted: 25 November 2013 / Published online: 10 December 2013

Abstract Due to the limit of nanofabrication methods of the nano-hole array (i.e., focused ion beam, nanoimprint/electron beam lithography, and metal film evaporation on top of the free standing membrane), the nano-hole arrays patterned in a noble metal film always has a non-vertical sidewall profile. In this work, the optical transmittance of the non-vertical profile nano-hole array with different tapered angle (α) and structural periodicity (P) was numerically investigated. The optimum tapered angle in case of positive profile of the nano-hole arrays was found as 10° and 12° at structural period of 450 and 500 nm, respectively. However, in case of negative profile, the optimum tapered angle of the nano-hole array was obtained as 4° at both structural period of 450 and 500 nm. The first and the second resonance modes of the nano-hole arrays with negative profile were shown a blueshift of 16 and 9 nm on increasing the tapered angle from 0° to 16° at structural period of 450 and 500 nm, respectively. It was also found that nano-hole arrays with positive tapered profile result in higher transmission than the negative profile one.

Keyword Surface plasmon resonance · Tapered sidewall profile · FDTD · Optical transmission · Nano-hole array

Introduction

Transmission enhancement of light through nanoscale hole or slit arrays in noble metal films has been an active research area back to 1998 when extraordinary transmission phenomenon was observed by Ebbesen et al. [1]. After Ebbesen's work, the optical properties of noble metals have been discussed by numerous authors [2–8], and many research works have been employed to reveal the physical origin of the light enhancement in nanostructures. Systematic reviews of this field have been given in review papers by Garcia de Abajo [9] and Garcia-Vidal et al. [10]. In nano-hole arrays (NHAs), the extraordinary optical transmission (EOT) phenomenon is attributed to the resonant excitation of surface plasmon polarition (SPP) which can be described as propagating electromagnetic surface waves and interference effect of propagating waves on both interfaces of the perforated holes in the optically thick metallic thin films[10, 11]. Surface plasmon is described as electromagnetic waves that are formed by charge oscillation at the metal/dielectric interface. The surface plasmon polarition has been defined as a waveguide mode since the self-consistency condition for the waveguide mode is naturally satisfied [12].

One main problem of fabricating nano-hole arrays in metallic thin films is the tapered (non-vertical) structure instead of vertical profile. There are three main methods that have been employed to pattern NHAs in a noble metal (e.g., Au or Ag) film; all of which lead to a tapered profile. The most popular method is focused ion beam (FIB) [13] milling of holes into the metal film, which is straightforward but with extremely low throughput and high cost. The milled profile is always tapered because of the broad "tail" of the finely focused beam and the degree of tapering depends on the beam current [14].

A more efficient method for EOT device fabrication is nanoimprint/electron beam lithography followed by a liftoff process [15] as shown in Fig. 1a. In this method, a thin layer of noble metal is coated by electron beam evaporation onto the polymer resist template. Dissolving the polymer thus lifting off the metal on top of it results in the desired EOT device. However, the profile is tapered due to the lateral deposition of the noble metal during evaporation. The third method involves the fabrication of free standing thin

M. Irannejad (✉) · J. Zhang · M. Yavuz · B. Cui
Waterloo Institute for Nanotechnology, University of Waterloo, Waterloo, Canada
e-mail: Mehrdad.Irannejad@uwaterloo.ca

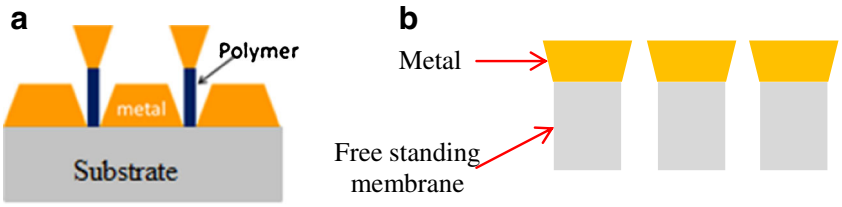

Fig. 1 Schematic diagram of a periodic array of tapered NHA that is fabricated by **a** nanoimprint/electron beam lithography in gold thin film placed on the glass substrate followed by a liftoff process that will dissolve the polymer pillar and liftoff the Au on top (positive tapered profile) and **b** evaporation of Au onto the hole array patterned on a free standing membrane (negative tapered profile). In both case of positive and negative profiles, the hole radius and hole depth both are 100 nm and tapered radius, R_{tap}, is given by Eq. 1

(i.e.,100 s nm) membrane having hole array pattern followed by evaporation of noble metal on top of it (Fig. 1b) [16–18]. Again, the profile is tapered due to the lateral deposition that gradually closes up the holes. Note that opposite to the pervious methods (i.e., FIB milling and nanoimprint/electron beam lithography which result in positive tapered profile), this method leads to a negative tapered profile (i.e., opening becomes smaller toward the top of the hole).

Optical transmission properties of tapered nanostructures such as tapered waveguide [19], V-grooves [20], trench nanostructure [21, 22] and double NHAs with slanted sidewalls [23] have been studied in the last decade. In a recent research, Søndergaard et al. [24] studied the EOT phenomenon in tapered slit with different slit height and tapered angle. They have found that the optimum taper angle was in the range of 6°–8°, and high resonant transmission was observed when Fabry–Parrot-like slit resonance was excited. It was reported that the highest transmission was achieved for fundamental resonance mode with smaller slit opening in one end even though more light could be collected by larger slit opening in the other end. The lower transmission can be explained as an effect of increased propagation loss and weaker slit resonance due to smaller reflection at the end of a wider slit.

In this work, we will study the effects of the tapered angle on the transmission of light through non-vertical cylindrical nano-hole using finite difference time domain (FDTD) technique. The NHA consists of thin gold film of thickness of 100 nm with period of 450 and 500 nm tapered angle (α) in the range of 0° to 16°, hole radius (R) of 100 nm, and tapered radius (R_{tap}) which is given by:

$$R_{tap} = R + 100 \times \tan(\alpha) \quad (1)$$

Methodology

Fabrication of NHA Using Double Liftoff Process

The nano-hole array fabrication was carried out using electron beam lithography (EBL) followed by double liftoff process on 2 in. fused silica substrate as shown in Fig. 2. A sacrificial layer of 400 nm poly(dimethyl glutarimide)(PMGI, MicroChem Corp.) was spin-coated on the substrate followed by 20 nm SiO_2 deposition by e-beam evaporation technique. Then, 90 nm layer of ZEP-520A was spin-coated as the positive resist layer followed by 10 nm Cr deposition as the conductive layer. EBL was carried out using Raith 150TWO system with 20 kV acceleration voltage 0.33 nA beam current (Fig. 2a). The Cr layer was dissolved using wet etching. The pattern was developed (Fig. 2b) using amyl acetate for 1 min and rinsed by isopropanol. A 10-nm Cr layer was deposited on the patterned sample (Fig. 2c) and soaked in anisole for 4 h for the first liftoff process. After first liftoff process, SiO_2 layer and PMGI layer were etched using reactive ion etching process with CF_4 and O_2, respectively (Fig. 2d). Finally, a 100-nm gold was deposited by e-beam evaporation (Fig. 2e), and the nano-hole arrays were fabricated by soaking the whole structure in AZ300 photoresist developer that dissolve PMGI for the second liftoff process (Fig. 2f).

Numerical Analysis

The effects of varying tapered angle on optical behavior of the incident EM field through the NHAs were analyzed using the 3D full wavevector FDTD method, which is a reliable method in solving Maxwell's equations in dispersive media like gold and silver. Each media was specified by relative permittivity, $\varepsilon(\omega)$. For glass and membrane layers, permittivity was assumed as $n^2(=1.45^2)$, and the Lorentz–Drude model was employed to describe the permittivity of film layer [25].

The FDTD was carried out using the commercial software package (FDTD solution 8) from Lumerical Inc. The plane wave source, nano-hole structure, and monitors were coplanar with boundary conditions that made them effectively infinite. In this study, a plane wave of wavelength in the range of 400 to 900 nm with electric field amplitude of 1 V/m which propagates in the z-axis was used. The asymmetric boundary condition in the x-direction and symmetric boundary condition in the y-direction and perfect matching layer (PML) in the z-direction was used to study the transmission properties at normal incident of electromagnetic wave through the sub-wavelength hole structure. The asymmetric and symmetric boundary conditions were considered in order to reduce the

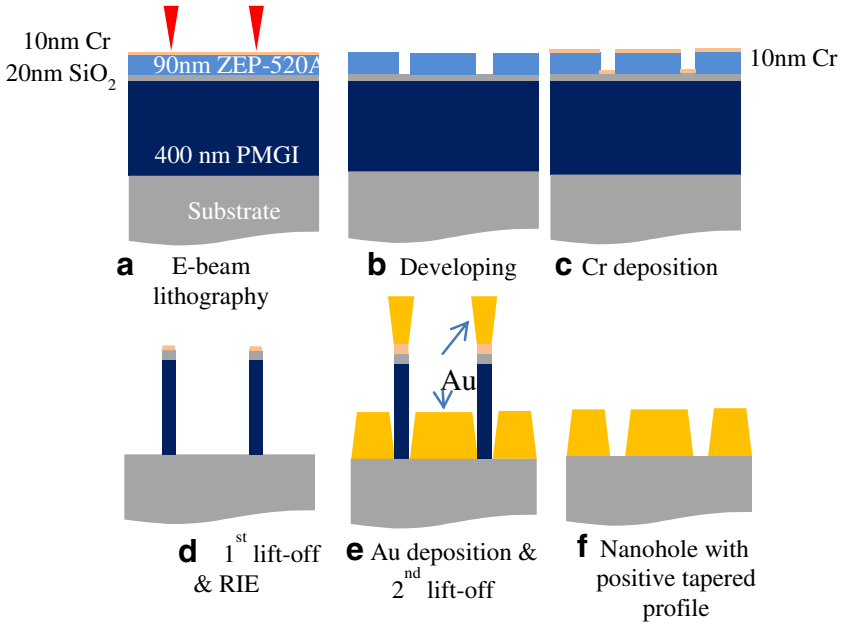

Fig. 2 Schematic diagram of the positive tapered profile nano-hole array fabrication procedure which includes **a** EBL process, **b** resist development, **c** Cr deposition, **d** first liftoff process and RIE, **e** gold deposition and second liftoff process, and **f** NHA with positive tapered profile. The hole radius and hole depth both are 100 nm, tapered radius and structural periodicity of the NHA are 118 and 500 nm, respectively

iteration time [26]. The calculation grid resolution was as high as 5 nm (grid point-to-point distance) in the simulation cell, and the conformal mesh method was used to calculating the electric and magnetic field at the corner and rounded region of the nano-holes. Although this method gives better convergence than staircasing method for small enough mesh sizes at larger mesh sizes, it could result worst results. In case of using metal and surface plasmon phenomena, the 5 nm or smaller mesh gird is sufficient [27, 28]. The calculation time was set to 100 fs, and the transmission spectra were calculated using an x–y monitor at 200 nm away from the air/Au interface. The incident electromagnetic field illuminated the structure from substrate medium through the NHA.

Results and Discussion

The optical behavior of circular NHAs with non-vertical profile was studied both experimentally and numerically. In the first structure, the tapered nano-holes were considered as results of lateral deposition of gold film by e-beam evaporation and liftoff process where upper surface of the nano-structures has larger radius than the bottom surface (positive profile) as it was shown in Fig. 3. In the second geometry, the tapered profile was due to the evaporation of gold film onto the hole array pattered on a free standing membrane of silica, which leads to smaller hole radius on the upper surface compared to the bottom one (negative profile).

NHA with Positive Profile

Here, the tapered nano-hole profile is due to lateral deposition of gold. Figure 4a shows the SEM micrograph of non-vertical profile NHAs of hole depth and hole radius of both 100 nm and structural periodicity of 500 nm fabricated by aforementioned technique. Measured and FDTD simulated transmission spectra of tapered nano-hole with tapered angle of 10° (Fig. 2a) were compared in Fig. 4b. As can be seen in this figure, except the transmission amplitude, a very good agreement in terms of peak position and overall trend between the FDTD result (red) and experimental one (black) was observed. The difference between the transmission amplitude of FDTD and measured values (black) might be due to the imperfection in the fabricated nano-hole structures such as roughness of the surface and edges which increases the light scattering and reduces the transmission intensity. The film roughness was reduced by annealing at 600 °C for 1 h as it was shown in Fig. 4a inset. The EOT measurement of the annealed NHA was also compared with FDTD and unannealed one in Fig. 4b. As can be seen from this figure, the transmission of the NHA after annealing (green) was improved, and the discrepancy between the FTDT and measurements was reduced.

Figure 4c, d shows transmission spectra of the tapered nano-hole with different tapered angle in the range of 0° to 16° with step of 4°, hole radius and hole depth of both 100 nm, and structural period of 450 and 500 nm. A broad peak around 490 nm with a transmission of 7 to 10 % (at different tapered angle) was observed in NHAs. This peak was attributed to the intraband transition (direct transmission) of gold film and occurs regardless of the NHAs structure and incident EM wave polarization [29, 30]. Another broad peak at wavelength of 625 nm (650 nm) with a transmission of 13 (17)% was also observed in the tapered NHAs of structural periodicity of 450 nm (500 nm) at tapered angle of 0°. This broad peak was attributed to the surface plasmon resonance mode of (1,1)

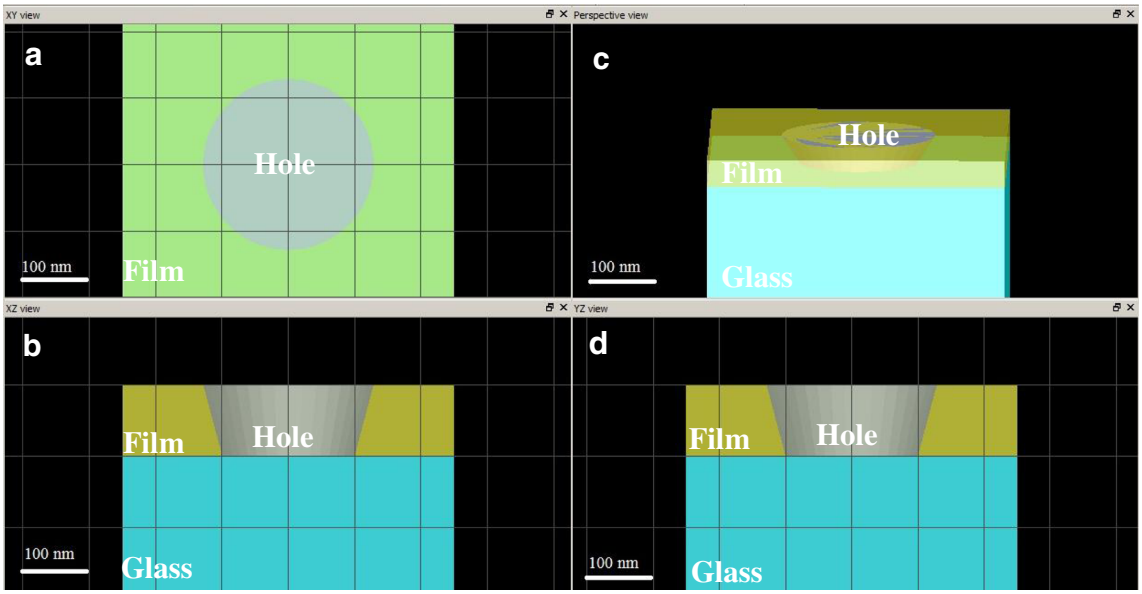

Fig. 3 The FDTD layout of positive profile NHA with hole radius and hole depth of both 100 nm, tapered angle of 16° and period of 500 nm in **a** *xy*-plane, **b** *xz*-plane, **c** perspective view, and **d** *zy*-plane

from Au/glass, which is close to the value predicted from dispersion equation [31] and reported in Table 1.

Figure 4c, d also shows antisymmetric sharp peak at wavelengths of 756 and 807 nm with transmission intensity of 50 and 48 % in the NHAs with tapered angle of 0° and structural periodicity of 450 and 500 nm, respectively, which is attributed to the SPP resonance mode of (1,0). The antisymmetric peaks were indicative of Fano resonance [32] which is a characteristic of interference between a resonant transmission and a non-resonant (Rayleigh anomaly) one and has been reported elsewhere [32–35]. The minimum in transmission spectra around the wavelengths of 710 and 770 nm, respectively, in Fig. 4c, d were ascribed to the Rayleigh anomaly (RA) which describes propagation of diffracted light waves in the plane of the surface and it is generally observed at wavelength given by [36]:

$$\lambda_{RA} = \frac{P}{(i^2 + j^2)^{1/2}} \sqrt{\varepsilon}$$

Where ε is the permittivity of the dielectric medium. As can be seen from Table 1, there is a moderate discrepancy in the range of 6 to 87 nm between the analytically calculated SPP wavelengths for both (1,0) and (1,1) resonance modes and FDTD calculated ones.

The normalized electric field ($|E/E_0|$) profile of the (1,0) resonance mode in the Au/glass interface at different tapered angle in the range of 0° to 16° with step of 4° and structural periodicity of 450 and 500 nm is shown in Fig. 5. From this figure, it is clear that normalized electric field confinement on the air/Au interface was very weak at these wavelength range (the SPP resonance peak of the air/Au interface has been reported at wavelength smaller than 500 nm [31]) which might be attributed to the electric field leakage to the air.

It is clear that the normalized electric filed confinement was reduced on increasing the tapered angle from 0° to 16° in the NHA with both period of 450 and 500 nm. It was also found that on increasing the tapered angle, the resonance peak position was shifted towards longer wavelength, whereas the transmission encountered non-monotonically change for both structural periodicity of 450 and 500 nm. The maximum value of $|E/E_0|$ was recorded on the vertical profile ($\alpha = 0°$) as 25 and 33 at wavelength of 756 and 807 nm in the NHA of period of 450 and 500 nm, respectively. The transmission intensity was reduced gradually to the minimum of 16 at tapered angle of 16°. The largest normalized electric field confinement of non-vertical NHA was recorded as 23 and 28 at tapered angle of 10° and 12°, respectively, as it is evident from Fig. 6.

The effect of increasing the tapered angle on the normalized near field electric field of the output surface was shown in Fig. 6 for structural period of 450 and 500 nm. As can be seen from this figure, the overall trend of the near field values was similar for both structural periods. The optimum tapered angle was obtained as 10° and 12° for structural periodicity of 450 and 500 nm, respectively, which was comparable to the reported values for the tapered nano-slit array [24]. The recorded value of the normalized electric field of the NHA of the tapered angle of 16° was observed in opposite direction of the overall trend (Fig. 6) for a period of 500 nm. This could be attributed to efficient tunneling of the excited SPP at the Au/glass interface through the nano-holes to the air/Au interface, where they are scattered plane waves and contribute to the light transmission as can be seen from Fig. 5j. From this

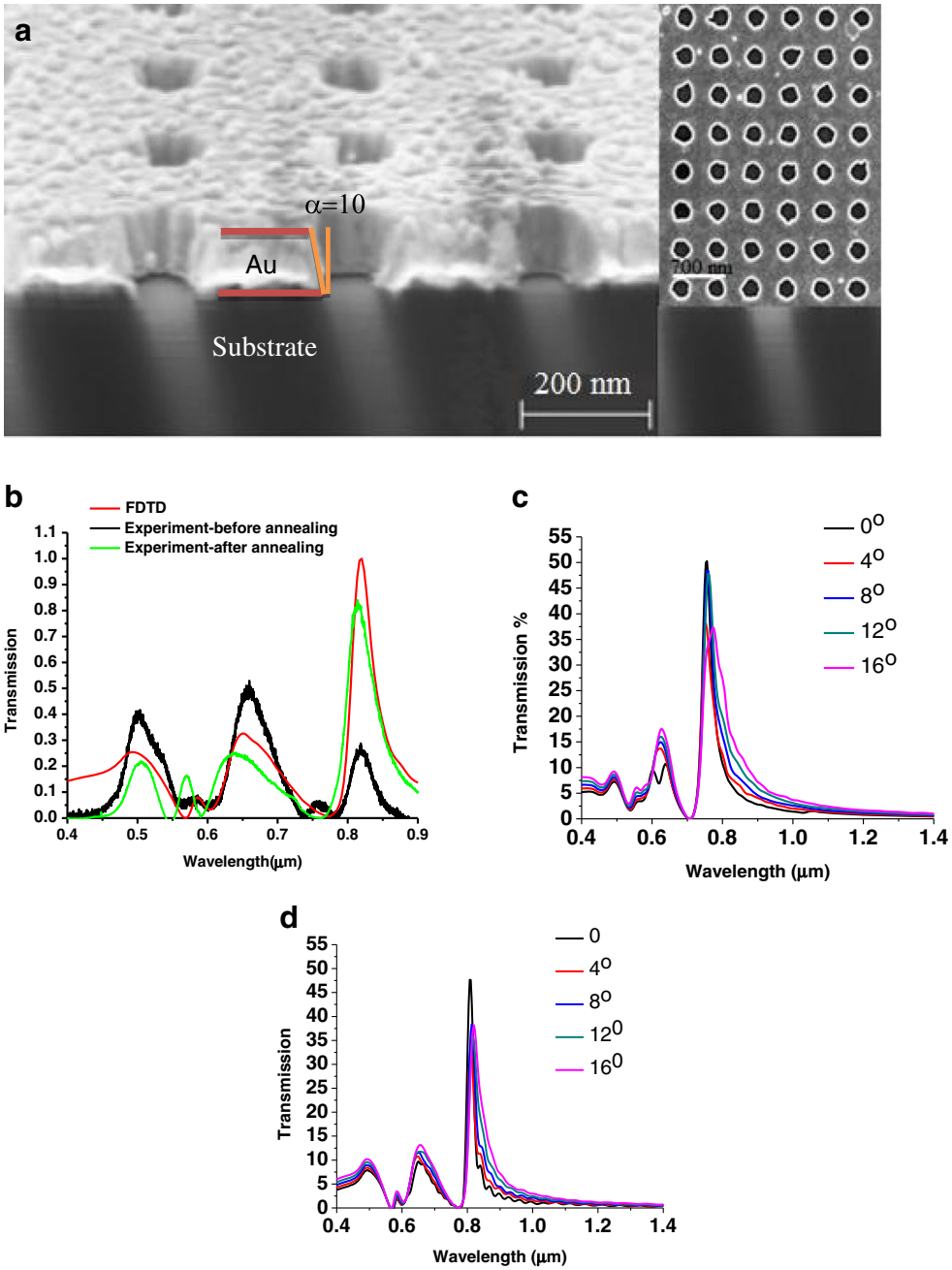

Fig. 4 **a** SEM micrograph of the positive profile NHA before annealing. The *inset* shows the positive profile NHA after annealing and **b** FDTD simulated transmission spectrum of the positive profile NHA and measured one before and after annealing at 600 °C. FDTD simulated near filed transmission spectrum of positive profile NHA of hole radius and hole depth of both 100 nm at different tapered angle and structural periodicity of **c** 450 and **d** 500 nm. Transmission in Fig. 2b is normalized to the hole area

figure, it can be observed that the normalized electric field value at the air/Au interface was recorded around 17.

NHAs with Negative Profile

As it was shown in Fig. 1b, in case of using hole array patterned on a free standing membrane as NHA substrate, the upper diameter was smaller than the bottom one. Figure 7a, b shows the FDTD calculated transmission spectra of the non-vertical NHAs placed on the silica membrane with hole radius and hole depth of both 100 nm and structural periodicity of 450 and 500 nm, respectively. The inset figures show the (1,0) SPP resonance peaks. As can be seen from Fig. 7, no significant changes were observed on the direct transmission peak position at wavelength of ~500 nm and its transmittance intensity on increasing the tapered angle from 0° to 16°, whereas a blueshift of 16 and 9 nm was recorded on SPP (1,0) and (1,1) resonance modes in the NHA of period of 450 and 500 nm, respectively. The transmission intensity was increased from 25 to 41 % on increasing the tapered angle for NHA of period of 450 nm.

This increase in the transmission intensity and blueshift in peak position could be attributed to the smaller surface area at the output (air/Au) interface of the NHA which results in

Table 1 Spectral position of SPP and RA on the Au/glass interface obtained from SPP dispersion equation which can be found elsewhere [31]

Order	SPP Wavelength (nm)		Order	RA Wavelength (nm)
	Analytically	FDTD		
P=450 nm				
1,0	762	756	1,0	652
1,1	538	625	1,0	461
P=500 nm				
1,0	847	807	1,0	725
1,1	598	556	1,1	512

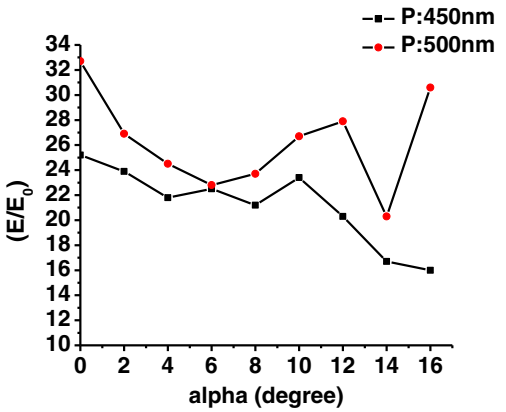

Fig. 6 Effect of tapered angle on the normalized electric field of the NHA of hole radius of 100 nm, hole depth of 100 nm, and period of 450 and 500 nm at wavelength of 820 and 200 nm away from the air/Au interface

focusing and shrinking the transmitted electromagnetic waves in the smaller area [37], while in NHA structure that was shown in Fig. 1a, the larger surface area at the output interface resulted in the distribution of the electromagnetic field in a larger area that leads to a redshift in the resonance peak position and reduction in the transmission intensity [24].

A weak transmission peak as shoulder was observed in the wavelength range of 800 nm (at α=16°) to 814 nm (at α=0) with transmission intensity in the range of 20.5 to 17 %, as it was clear from Fig. 7a. This transmission peak could be attributed to the localized SPP which contributed to the (1,0) SPP resonance mode. In addition, the (1,1) resonance mode from Au/glass interface and the (1,0) resonance mode of the air/Au interface interfered to result in the broad peak at wavelength of 602 and 631 nm for structural periodicity of 450 and 500 nm, respectively. However, for 0° tapered angle, the two modes were observed as separate transmission peaks.

Figure 8 shows near-filed profile of normalized electric field of the (1,0) resonance mode at the Au/glass interface at different tapered angles in the range of 0° to 16° with step of 4° and period of 450 and 500 nm. It was found that by fabricating the non-vertical nano-hole array on the silica membrane, the surface plasmon resonance were excited on both air/Au and Au/glass interfaces as it was evident from Fig. 8, which its strength and confinement decreased on increasing the tapered angle from 0° to 16°.

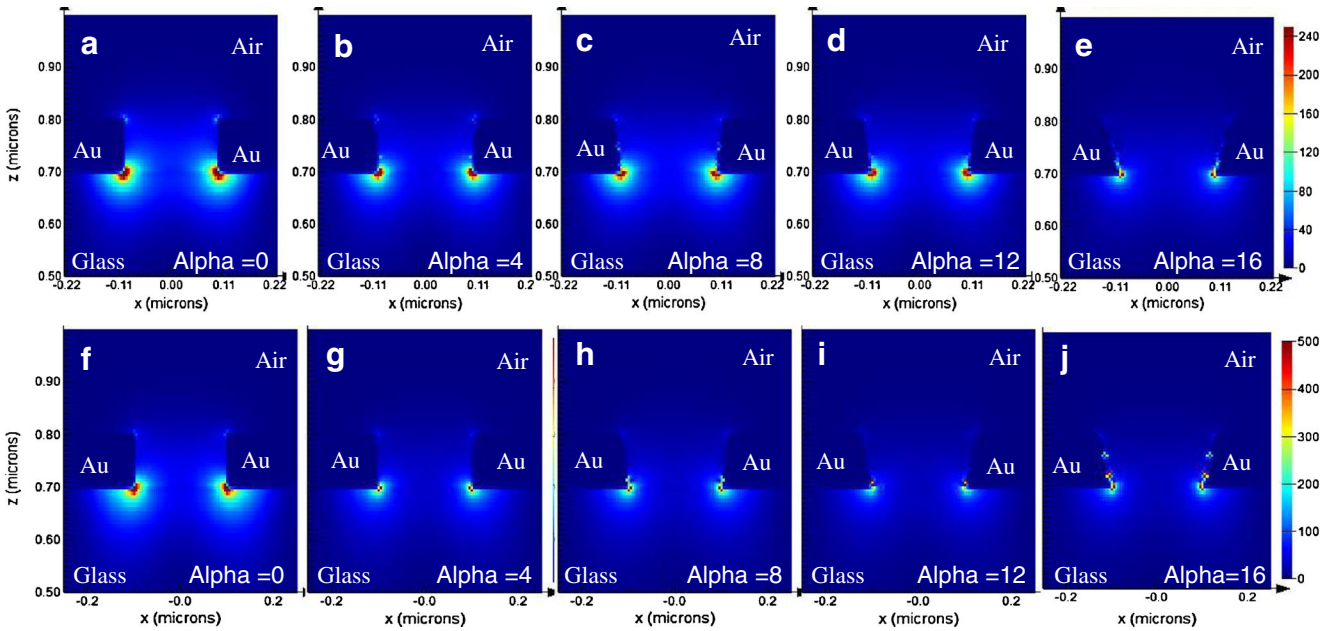

Fig. 5 The FDTD calculated $|E/E_0|^2$ profile of the $(1,0)_{Au/glass}$ resonance mode. The *top row* shows the cross-section across the middle of the tapered nano-holes of 450 nm period at wavelength of **a** λ=756 nm and α=0°, **b** λ=753 nm and α=4°, **c** λ=759 nm and α=8°, **d** λ=759 nm and α=12°, and **e** λ=771 nm and α=16°. The *bottom row* is for tapered nano-holes of 500 nm period at wavelength of **f** λ=807 nm and α=0°, **g** λ=810 nm and α=4°, **h** λ=814 nm and α=8°, **i** λ=817 nm and α=12°, and **j** λ=820 nm and α=16°. The hole radius and hole depth are both 100 nm. Light incident from the substrate medium through the NHA

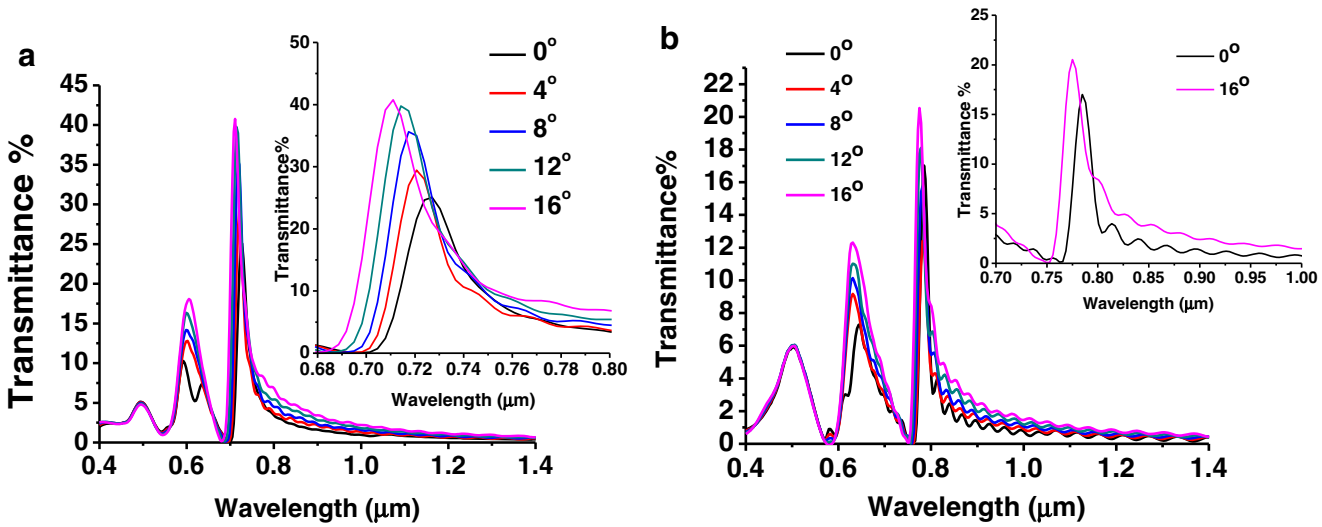

Fig. 7 FDTD calculated optical transmission spectrum of the non-vertical profile NHA placed on the silica membrane at different tapered angle, hole depth, and hole radius of both100 nm and periodicity of **a** 450 and **b** 500 nm

Conclusion

The optical behavior of the non-vertical profile NHA placed on the silica substrate and silica membrane with different tapered angle in the range of 0° to 16°was studied. It was shown that on increasing the tapered angle, the (1,1) SP mode of the Au/glass interface and (1,0) SP mode of the air/Au interfaces interfered to result in weak shoulder peak. It was shown that fabrication of the nano-hole array using Au evaporation and liftoff process results in higher transmission than direct deposition of Au on the free standing membrane. The near-field electric filed confinement of both structure at period of 450 and 500 nm were studied and the optimum tapered angle was found as 4° with maximum normalized electric field of 13.5 and 11.8 in the NHAs placed on the silica membrane at period of 450 and 500 nm, respectively. Whereas on using the silica glass as NHA substrate, the maximum normalized electric field enhancement of 23 and 28 were recorded at tapered angle of

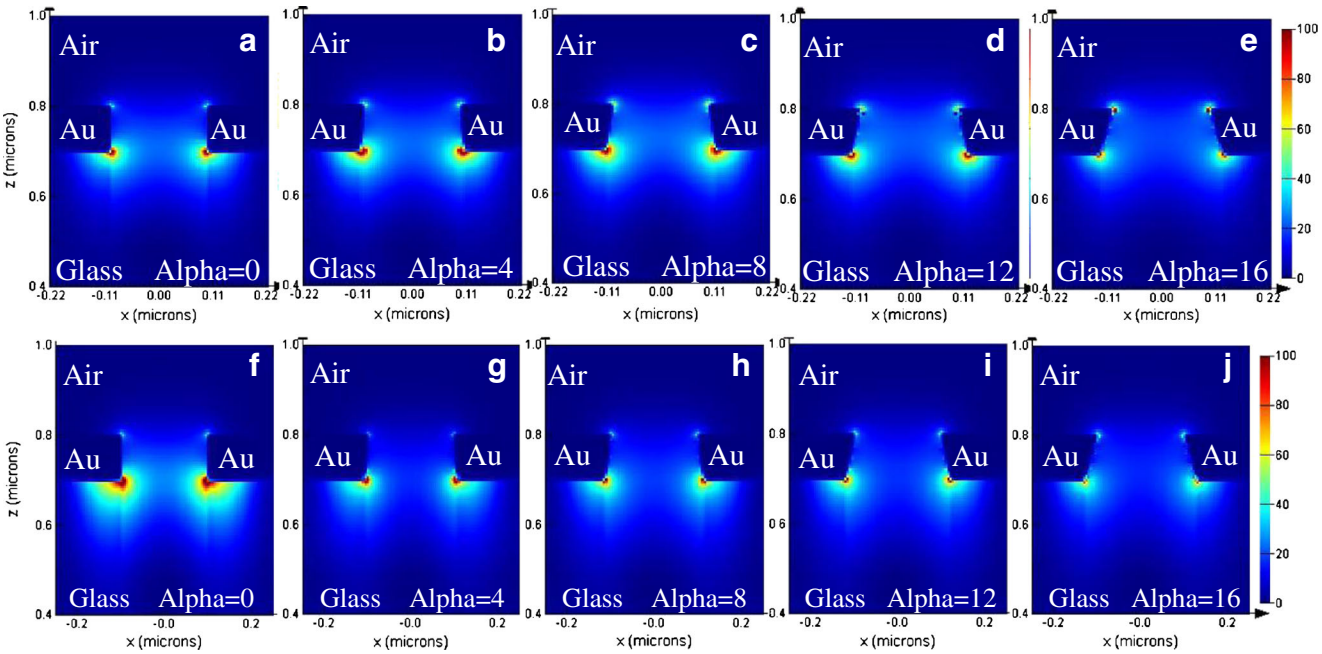

Fig. 8 The FDTD calculated $|E/E_0|^2$ profile of the $(1,0)_{Au/glass}$ resonance mode. The *top row* shows the cross-section across middle of the tapered nano-holes of 450 nm period at wavelength of **a** $\lambda = 727$ nm and $\alpha = 0$, **b** $\lambda = 721$ nm and $\alpha = 4°$, **c** $\lambda = 717$ nm and $\alpha = 8°$, **d** $\lambda = 714$ nm and $\alpha = 12°$, and **e** $\lambda = 711$ nm and $\alpha = 16°$. The *bottom row* is for 500 nm period at wavelength of **f** $\lambda = 784$ nm and $\alpha = 0$, **g** $\lambda = 781$ nm and $\alpha = 4°$, **h** $\lambda = 781$ nm and $\alpha = 8°$, **i** $\lambda = 778$ nm and $\alpha = 12°$, and **j** $\lambda = 775$ nm and $\alpha = 16°$. The hole radius and hole depth were both 100 nm. Light incident from the substrate medium through the NHA

10° and 12° in the NHA with structural period of 450 and 500 nm, respectively. The first and the second resonance modes of the NHAs on the silica membrane show a blueshift of 16 and 9 nm on increasing the tapered angle from 0° to 16° at structural periodicity of 450 and 500 nm, respectively.

Acknowledgments The authors acknowledge the National Science and Engineering Research Council of Canada (NSERC) for their financial support (Ref# EGP 445290–12). The authors acknowledge Prof. Simarjeet Saini and Mr. Jaspreet Walia for transmission measurement of the tapered NHAs.

References

1. Ebbesen TW, Lezec HJ, Ghaemi HF, Thio T, Wolff PA (1998) Extraordinary optical transmission through sub-wavelength hole arrays. Nature 391(6668):667–669
2. Vial A, Laroche T, Dridi M, Le Cunff L (2011) A new model of dispersion for metals leading to a more accurate modeling of plasmonic structures using the FDTD method. Appl Phys A 103(3):849–853. doi:10.1007/s00339-010-6224-9
3. Hess O, Pendry JB, Maier SA, Oulton RF, Hamm JM, Tsakmakidis KL (2012) Active nanoplasmonic metamaterials. Nat Mater 11(7):573–584
4. Tang ZH, Peng RW, Wang Z, Wu X, Bao YJ, Wang QJ, Zhang ZJ, Sun WH, Wang M (2007) Coupling of surface plasmons in nanostructured metal/dielectric multilayers with subwavelength hole arrays. Phys Rev B 76(19):195405
5. Vial A, Laroche T (2007) Description of dispersion properties of metals by means of the critical points model and application to the study of resonant structures using the FDTD method. J Phys D Appl Phys 40:7152–7158
6. Xiao S, Mortensen NA, Qiu M (2007) Enhanced transmission through arrays of subwavelength holes in gold films coated by a finite dielectric layer. J Eur Opt Soc-Rapid Publ 2:07009
7. Guo J, Adato R (2006) Extended long range plasmon waves in finite thickness metal film and layered dielectric materials. Opt Express 14(25):12409–12418
8. Coe JV, Heer JM, Teeters-Kennedy S, Tian H, Rodriguez KR (2008) Extraordinary transmission of metal films with arrays of subwavelength holes. Annu Rev Phys Chem 59(1):179–202. doi:10.1146/annurev.physchem.59.032607.093703
9. García de Abajo FJ (2007) Colloquium: light scattering by particle and hole arrays. Rev Mod Phys 79(4):1267–1290
10. Garcia-Vidal FJ, Martin-Moreno L, Ebbesen TW, Kuipers L (2010) Light passing through subwavelength apertures. Rev Mod Phys 82(1):729–787
11. Liu H, Lalanne P (2008) Microscopic theory of the extraordinary optical transmission. Nature 52(7188):728–31. doi:10.1038/nature06762
12. Gordon R (2008) Surface plasmon nanophotonics: a tutorial. Nanotechnol Mag IEEE 2(3):12–18. doi:10.1109/mnano.2008.931481
13. Lovera P, Jones D, Corbet B, O'Riordan A (2012) Polarization tunable transmission through plasmonic arrays of elliptical nanopores. Opt Express 20(23):25325–25332
14. Anguita J, Alvaro R, Espinosa F (2012) A new experimental method to obtain the ion beam profile of focused ion beam nanotechnology systems. Int J Mech Eng Mechatron 1(1):61–65
15. Jung WK, Byun KM (2011) Fabrication of nanoscale plasmonic structures and their applications to photonic devices and biosensors. Biomed Eng Lett 1:153–162
16. Takeda S, Koto K, Iijima S, Ichihashi T (1997) Nanoholes on silicon surface created by electron irradiation under ultrahigh vacuum environment. Phys Rev Lett 79(16):2994–2997
17. Bysakh S, Shimojo M, Mitsuishi K, Furuya K (2004) Mechanisms of nano-hole drilling due to nano-probe intense electron beam irradiation on a stainless steel. J Vac Sci Technol B: Microelectron Nanomet Struct 22(6):2620–2627
18. Wu M-Y, Krapf D, Zandbergen M, Zandbergen H, Batson PE (2005) Formation of nanopores in a SiN/SiO[sub 2] membrane with an electron beam. Appl Phys Lett 87(11):113106–113103
19. Stockman MI (2004) Nanofocusing of optical energy in tapered plasmonic waveguides. Phys Rev Lett 93(13):137404
20. Bozhevolnyi SI, Volkov VS, Devaux E, Ebbesen TW (2005) Channel plasmon-polariton guiding by subwavelength metal grooves. Phys Rev Lett 95(4):046802
21. Bozhevolnyi SI (2006) Effective-index modeling of channel plasmon polaritons. Opt Express 14(20):9467–9476
22. Gramotnev DK, Pile DFP, Vogel MW, Zhang X (2007) Local electric field enhancement during nanofocusing of plasmons by a tapered gap. Phys Rev B 75(3):035431
23. Shahmansouri A, Rashidian B (2013) Enhanced optical transmission through metallic holes array: role of the polarization in SPP excitation. Plasmonics 8(2):403–409. doi:10.1007/s11468-012-9404-y
24. Søndergaard T, Bozhevolnyi SI, Beermann J, Novikov SM, Devaux E, Ebbesen TW (2012) Extraordinary optical transmission with tapered slits: effect of higher diffraction and slit resonance orders. J Opt Soc Am B 29(1):130–137
25. Rakic AD, Djurisic AB, Elazar JM, Majewski ML (1998) Optical properties of metallic films for vertical-cavity optoelectronic devices. Appl Opt 37(22):5271–5283
26. Lumerical, Symmetric and anti-symmetric boundary condition. http://docs.lumerical.com/en/fdtd/user_guide_symmetric_anti_symmetric.html.
27. Lumerical, Mesh refinement options. http://docs.lumerical.com/en/fdtd/user_guide_mesh_refinement_options.html.
28. Lumerical, Mesh refinement. http://docs.lumerical.com/en/fdtd/user_guide_mesh_refinement.html.
29. Gao H, Henzie J, Odom TW (2006) Direct evidence for surface plasmon-mediated enhanced light transmission through metallic nanohole arrays. Nano Lett 6(9):2104–2108. doi:10.1021/nl061670r
30. Irannejad M, Cui B (2013) Effects of refractive index variations on the optical transmittance spectral properties of the nano-hole arrays. Plasmonics 8(2):1245–1251. doi:10.1007/s11468-013-9540-z
31. Ghaemi HF, Thio T, Grupp DE, Ebbesen TW, Lezec HJ (1998) Surface plasmons enhance optical transmission through subwavelength holes. Phys Rev B 58(11):6779–6782
32. Miroshnichenko AE, Flach S, Kivshar YS (2010) Fano resonances in nanoscale structures. Rev Mod Phys 82(3):2257–2298
33. Francescato Y, Giannini V, Maier SA (2012) Plasmonic systems unveiled by fano resonances. ACS Nano 6(2):1830–1838. doi:10.1021/nn2050533
34. Luk'yanchuk B, Zheludev NI, Maier SA, Halas NJ, Nordlander P, Giessen H, Chong CT (2010) The Fano resonance in plasmonic nanostructures and metamaterials. Nat Mater 9(9):707–715
35. Rahmani M, Lukiyanchuk B, Ng B, Tavakkoli KGA, Liew YF, Hong MH (2011) Generation of pronounced Fano resonances and tuning of subwavelength spatial light distribution in plasmonic pentamers. Opt Express 19(6):4949–4956
36. Gao H, McMahon JM, Lee MH, Henzie J, Gray SK, Schatz GC, Odom TW (2009) Rayleigh anomaly-surface plasmon polariton resonances in palladium and gold subwavelength hole arrays. Opt Express 17(4):2334–2340
37. Bouhelier A, Renger J, Beversluis MR, Novotny L (2003) Plasmon-coupled tip-enhanced near-field optical microscopy. J Microsc 210(3):220–224. doi:10.1046/j.1365-2818.2003.01108.x